.

PROCESS AND REACTOR DESIGN FOR THERMO-CHEMICAL ENERGY STORES

Barbara Mette, Henner Kerskes, Harald Drück

University of Stuttgart, Institute for Thermodynamics and Thermal Engineering (ITW)
Research and Testing Centre for Thermal Solar Systems (TZS)
Pfaffenwaldring 6, 70550 Stuttgart, Germany
Tel.: +49 711 / 685-63499, Fax: +49 711 685-63503
email: mette@itw.uni-stuttgart.de

1. Introduction

Thermo-chemical energy storage is a key technology to realize highly efficient short and long term thermal energy stores for various applications such as solar thermal systems or cogeneration systems. By storing the energy in form of chemical bonds of special materials the energy can be stored almost loss-free over arbitrary time periods. At the same time a high energy storage density can be achieved. Both criteria are crucial, especially for compact long term thermal energy storage applications.

Research activities in the field of low temperature thermo-chemical energy stores (TCES) have developed strongly in the last few years - particularly in the field of material development and material optimization. Main focus of this activity is on improving the chemical and thermal properties of the materials such as increasing the energy storage density, enhancing the thermal conductivity or improving the cycle stability. Much less attention is paid to the design of the storage itself and its sub-components such as the reactor required as a key component in a thermo-chemical energy store. Nevertheless, this topic is indispensable to advance and push the developments of this technology and to bring it closer to a market introduction.

Hence, one focus of the work performed at the Institute for Thermodynamics and Thermal Engineering (ITW) of the University of Stuttgart is the development and integration of a thermo-chemical energy store into a complete system concept. Within the three and a half years project "Chemical heat store using reversible gas solid reactions (CWS: Chemische Wärmespeicherung mittels reversibler Feststoff-Gasreaktionen; duration from June 2008 to November 2011) a process design for integrating a thermo-chemical energy store into a solar combisystem is being developed. An essential aspect of the process development was the designing of the reactor and of the reaction conditions. This work has been closely accompanied by material research as, for an optimal utilization of the materials storage density, reaction behaviour and reactor design have to be specially adapted to the material characteristic and to the operation conditions of the system. Within the project, a wide range of materials for thermo-chemical energy stores have been experimentally investigated. In the focus are reversible gas solid reactions with water vapour as one reactant. Very good characteristics in terms of energy storage density and reaction kinetics indicate composite materials of salt impregnated zeolites. However, the reaction kinetic of these composites is instationary (decreasing kinetic with increasing conversion) and strongly dependent on the reaction conditions. This is a challenge especially for the exothermic formation reaction. To make use of the complete energy storage density of the material, it is essential to achieve a maximum conversion of the material with a temperature lift in the reactor which can be used for space heating and hot water preparation.

Different reactor designs have been experimentally and numerically investigated. For a detailed analysis of the heat and mass transfer inside the reactor a finite element model of the reactor has been set up with the simulation software "COMSOL Multiphysics"' (Comsol, 2010). The results of the numerical investigation will be presented as well as the derived reactor design for a thermo-chemical energy store. A very detailed overview of the newly developed process design, the CWS-NT-Concept (Chemische Wärmespeicherung - Niedertemperatur: chemical heat storage - low temperature) as well as the energy performance of the CWS-NT-concept will be given in (Kerskes et al., 2011b).

2. Process and reactor design

Figure 1 shows a schematic of the CWS-NT-concept: a thermo-chemical energy store is integrated in a solar combisystem. The collector loop of the solar combisystem has been extended for the thermo-chemical energy store. In times of high solar irradiation the heat coming from the collector array is directly charging the combistore or, if the temperature in the combistore is above the set temperature, regenerating the material in the thermo-chemical energy store (left figure). During winter or during times of low solar irradiation the thermo-chemical energy store is delivering heat for charging the combistore (right figure). The (conventional) backup heater is only used in extreme situation (long periods without solar radiation and/or very low ambient temperatures) as a kind of emergency heater

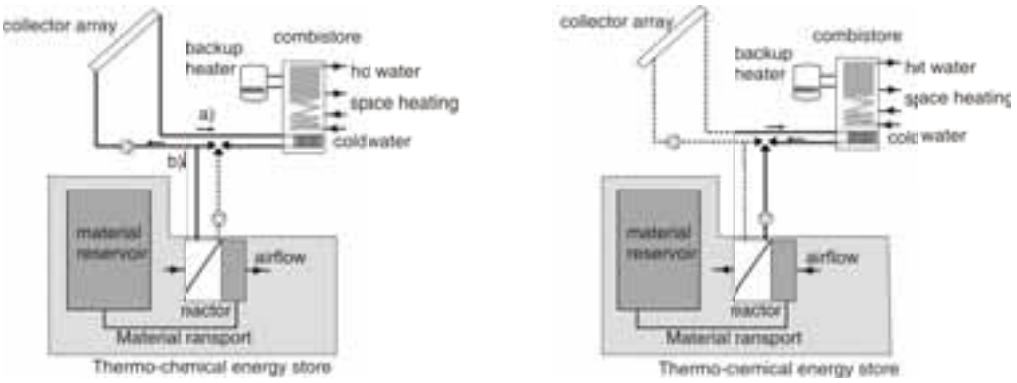

Fig. 1: Schematic of the CWS-NT-concept. Left: Solar collectors are delivering heat for charging the combistore (a) or regenerating the thermo-chemical energy store (b). Right: Thermo-chemical energy store is delivering heat for charging the combistore.

The thermo-chemical energy store has to fulfil two functions. It must provide a storage reservoir for the material and a reactor where the heat and mass transfer take place during the endothermic or exothermic reaction. For simplicity, the term "reaction" is used to describe sorption, hydration or a combination of both processes. During the exothermic reaction a solid reactant A reacts with water vapour to a solid product B and the reaction enthalpy ΔH_R is released. For the endothermic reaction the reaction enthalpy ΔH_R has to be added to the process in the form of heat and the product B is decomposed into the solid reactant A and water (H_2O); cf. eq. 1.

$$A_{(s)} + H_2O_{(g)} \rightleftharpoons B_{(s)} + \Delta H_R \qquad \text{(eq. 1)}$$

Water in vaporized form is supplied to the reactor (exothermic reaction) or dissipated from the reactor (endothermic reaction) through an airflow using ambient or exhaust air. Beside the water vapour transport, the airflow is also transporting the heat into the reactor (endothermic reaction) or out of the reactor (exothermic reaction). This has the advantage that despite the low conductivity of the material bed a very good heat transport mainly based on forced convection can be achieved.

Two different designs of thermo-chemical energy stores have been investigated at ITW: an integrated reactor concept where the material storage is at the same time the reactor (figure 2 left) and an external reactor concept where the material storage is separated from the reactor (figure 2 right). Both concepts have advantages and disadvantages.
In the integrated reactor concept the material is stationary inside the storage. A material transport is not required meaning less material stress as well as non technical or energetic effort for transporting the material. On the other hand, high temperatures ($\vartheta > 120\,^{\circ}\mathrm{C}$) are needed for the endothermic regeneration reaction. This implies the use of temperature resistant materials throughout the entire thermo-chemical energy store.
In the external reactor concept the material is transported between the reactor and the material storage. This requires an abrasion-resistant and transportable material. The advantage of the external reactor concept is that the reaction is reduced to only a small part of the total material amount at a time. The thermal heat capacities and heat losses especially during the regeneration process are reduced. Furthermore, only the reactor has to withstand high temperatures whereas for the material storage low-cost materials can be used.

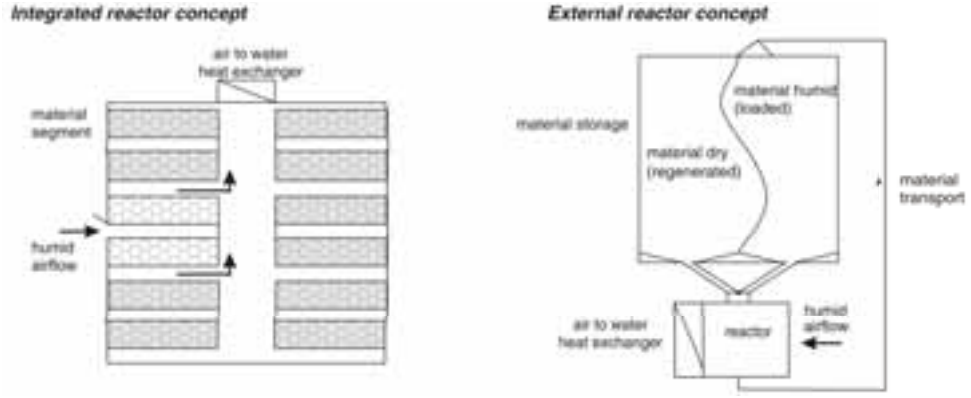

Fig. 2: Integrated (left) and external (right) reactor concept for a thermo-chemical energy store (example of the exothermic reaction).

In the following the external reactor concept will be described in more detail. Nevertheless, the integrated reactor concept is also subject of current research activities at ITW.

3. The external reactor design

In figure 3, left the schematic of the air circuit is given. An important element for an efficient process design is the air to air heat exchanger where the air coming from the reactor is preheating the supply air. A very low temperature difference between the air entering the reactor and the exhaust air is achieved; hence heat losses through the airflow are minimized.
The two right figures show the reactor design in more detail. The material is entering the reactor from top and runs gravity-driven through the reactor. The air is entering the reactor from lateral through a special designed air duct in order to achieve a uniform airflow over the reactor width. During the exothermic reaction the airflow is transporting the water vapour into the reactor and the heat of reaction out of the reactor. In the air to water heat exchanger the heat is transferred to the water loop. For the endothermic reaction the airflow direction is reversed. The heat from the solar loop is transferred to the airflow via the air to water heat exchanger and then transported into the reactor. The water vapour released during the reaction is transported with the airflow out of the reactor.

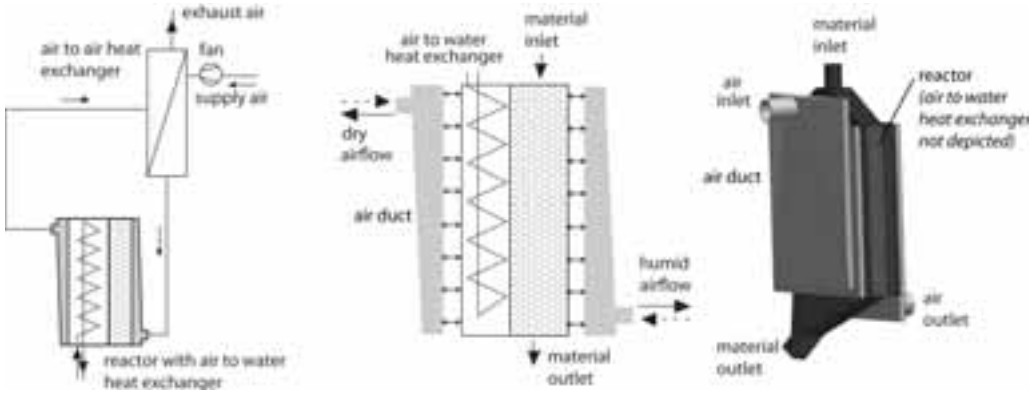

**Fig. 3: Left: Schematic of the air circuit .
Middle and right: Schematic of the external reactor design**

The following considerations were decisive for the derived reactor design:

- A large cross-flow section area for the airflow and a minimal material width in flow direction minimize the airflow pressure loss. This is essential for a low fan power required for the air transport.
- The material transport through the reactor can be realized in a reliable and technical inexpensive way with low material stress

- A compact construction with short distance between heat source and heat removal, i.e. between reaction chamber and heat exchanger, is favourable to minimize heat losses to the ambient.

The reactor can be operated as a cross flow or fixed bed reactor reactor. The main characteristics of the two different concepts will be briefly discussed. A more detailed assessment is given in section 5. where the different concepts are compared on the basis of numerical investigations.

The cross flow reactor
In the cross flow reactor the material runs from top to bottom gravity-driven through the reactor. The air is fed into the reactor from lateral and flowing in cross flow to the material. This reactor design allows a reaction process with a stationary reaction zone and a stationary thermal power output. A challenge of the reactor design is the realization of a uniform material flow through the reactor. This is essential as an inhomogeneous flow or even a funnel flow with stagnant zones in the reactor will significantly reduce the thermal performance and the thermal efficiency of the reactor.

The fixed bed reactor
In a fixed bed reactor the material is stationary inside the reactor and air is flown through the material bed. The reaction front and simultaneously the temperature and conversion front are moving through the reactor, starting at the airflow inlet. When full conversion of the material is achieved the material in the reactor has to be replaced. Due to the semi-batch operation of the reactor no constant thermal power output can be provided at the reactor outlet; a power reduction at start-up and the end of conversion is expected. An advantage of such a design is that the material is stationary inside the reactor during the reaction and no technical measures for a uniform material flow are required.

4. Experimental investigation of materials for thermo-chemical energy stores

Different materials and material combinations for thermo-chemical energy stores are being experimentally investigated at ITW. The investigations are performed in a fixed bed reactor (material volume of approximately 130 ml) flown through by a humid airflow (exothermic reaction) or a dry and heated airflow (endothermic reaction). Experiments have been conducted with pure salts such as magnesium sulphate or calcium chloride as well as salts on different carrier matrices (e.g. bentonite, zeolite). A detailed overview of the experimental setup and results are given e.g. in (Kerskes et al., 2011a) and (Bertsch et al., 2010).

Very good characteristics in terms of reaction kinetic, energy storage density and mechanical stability were observed for composite materials of salt impregnated zeolites. These materials are made by impregnating commercially available zeolites (e.g. zeolite 13X or zeolite 4A particles). The salt remaining on the particles after drying is mainly distributed over the inner surface of the zeolite so that there is no volume increase due to impregnation. Figure 4 shows an example of an exothermic reaction of zeolite 13X and a composit material conducted in the experimentel setup. The composite material was developed at ITW and consists of zeolite 13X which has been impregnated with approximately 9 mass percent of magnesium sulphate and 1 mass percent of lithium chloride. Depicted are the temperature $\vartheta_{\mathrm{f,in}}$ and $\vartheta_{\mathrm{f,out}}$ and the water vapour pressure $p_{\mathrm{w,in}}$ and $\mathrm{p_{w,out}}$ of the airflow at the reactor inlet and outlet. The experiments have been performed with a material volume of approximately 130 ml, corresponding to a material mass of $\mathrm{m} = 86\,\mathrm{g}$ of zeolite and $\mathrm{m} = 95\,\mathrm{g}$ of composite material. The particle size of the zeolite and composite varies between 1.5 mm and 2 mm.
The exothermic reaction has been performed at an inlet temperature of the airflow of $\vartheta_{\mathrm{f,in}} = 35^{\circ}\,\mathrm{C}$ and a water vapour pressure of $p_{\mathrm{w,in}} = 20\,\mathrm{mbar}$. Prior to the exothermic reaction the materials have been regenerated in the reactor at an inlet temperature of the airflow of $\vartheta_{\mathrm{f,in}} = 180^{\circ}\,\mathrm{C}$ and a water vapour pressure of the airflow of $p_{\mathrm{w,in}} \approx 1\,\mathrm{mbar}$.
Despite the additional salt concentration on the composite and hence additional hydration capacity of the composite the overall water uptake during the exothermic reaction does not increase compared to pure zeolite. The measured weight increase over the reaction was approximately $\Delta\mathrm{m} = 20\,\mathrm{g}$ resulting in a relative water uptake (related to the regenerated material mass) of 23 % for zeolite 13X and 21 % for the composite. Theoretically, assuming an unchanged adsorption capacity of the zeolite and a full hydration of the salt, a fractional water loading of 27 % is possible for the composite. Hence, only about 70 % of the theoretically possible water uptake is achieved in the experiment.

The course of the water vapour pressure of the outlet airflow $p_{\mathrm{w,out}}$ is very similar during the experiment for both materials. This might indicate a similar reaction kinetic. On the other hand, the reactor outlet temperature of the airflow measured over the reaction time, is higher for the composite than for the zeolite 13X. Reason for this might be a higher heat of reaction due to the salt reaction. In total, the heat released during the reaction is approximately 20 % higher for the composite compared to the pure zeolite.

For a more detailed characterization of the materials, both materials were analysed by nitrogen adsorption at 77 K with a volumetric sorption analyser (performed at "Institut für Nichtklassische Chemie", University of Leipzig, Germany). The specific surface area and specific pore volume have been determined from the isotherms by applying the Brunauer-Emmett-Teller (BET) equations (Brunauer et al., 1938). In figure 5 the N_2-isotherms at 77 K for zeolite 13X and the composite are depicted. The shape of the curve is similar but the isotherm of the composite is significantly lower than the isotherm of the pure zeolite. In absolute values, the pore volume of the composite is reduced by 26.5 % and the specific surface area by 32.7 %. This leads to the conclusion that the salt is blocking some of the pores so that not all zeolite crystals are available for adsorption. However, the experiments performed in the fixed bed reactor show an unchanged water uptake of the composite. Possible reasons for this is that the salt hydration is compensating the reduced adsorption capacity of the zeolite and/or the water molecules can pass the pores which are blocked for nitrogen. A further material characterization is planned to investigate the adsorption and hydration behaviour in more detail. It is expected that with a further improvement of the zeolite structure and impregnation technique a significant increase in the storage density of the materials can be achieved.

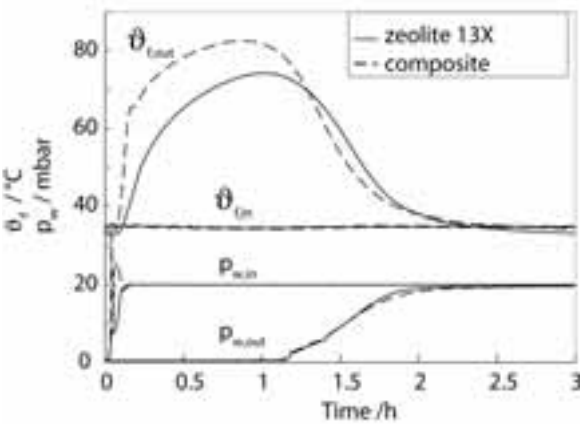

Fig. 4: Reaction of zeolite and composite: Airflow temperatures (ϑ_{in} and ϑ_{out}) and water vapour pressures ($p_{\mathrm{w,in}}$ and $p_{\mathrm{w,out}}$) measured at the reactor inlet and outlet

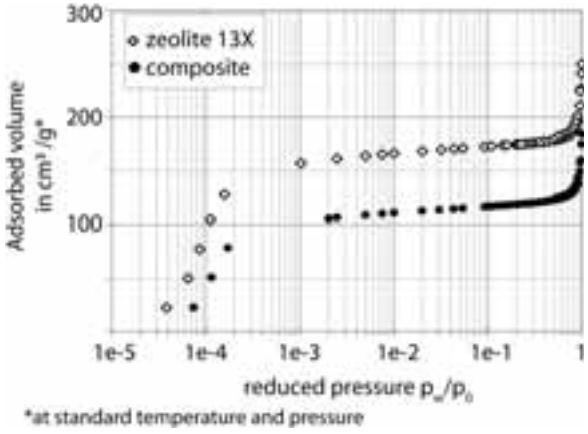

Fig. 5: N_2 - isotherms at 77 K for zeolite 13X and composite

5. Numerical investigation of external reactor designs

A detailed two-dimensional numerical model of the heat and mass transfer inside the reactor has been set up with the finite element simulation software "COMSOL Multiphysics". The aim was to investigate different reactor designs such as a cross flow and fixed reactor in more detail.

5.1. Governing equations

The mass balance of the water vapour in the fluid (air) is described by the following equation:

$$\epsilon \frac{\partial y_w}{\partial t} = D_{\mathrm{eff}} \frac{\partial^2 y_w}{\partial x_i^2} - u_{f,0,i} \frac{\partial y_w}{\partial x_i} + \epsilon R_w \qquad \text{(eq. 2)}$$

In the equation ϵ is the porosity of the bed, y_w the absolute humidity of the air, t the time, D_{eff} the effective mass dispersion coefficient, $u_{f,0,i}$ the superficial velocity of the airflow in i-direction, R_w the

reaction rate of the water vapour and x_i the coordinate in i-direction (i = 1, 2).

The conversion of the solid is described by:

$$(1-\epsilon)\ \frac{\partial y_s}{\partial t} = -u_{s,0,i}\ \frac{\partial y_s}{\partial x_i} + (1-\epsilon)\ R_s \qquad \text{(eq. 3)}$$

In the equation y_s is the conversion of the solid, $u_{s,0,i}$ the bulk velocity of the solid in i-direction and R_s the reaction rate of the solid. The correlation between R_s and R_w is given with:

$$R_w = -R_s\ \frac{\rho_{s,0}}{\rho_f}\ \frac{(1-\epsilon)}{\epsilon} \qquad \text{(eq. 4)}$$

with $\rho_{s,0}$ as density of the solid at $y_s = 0$ and ρ_f as the density of the fluid, which is considered to be constant during the reaction.

Under the assumption of a small temperature difference between solid and air inside of the reactor, a quasi-homogeneous model can be applied to describe the energy transport:

$$\epsilon\ \frac{\partial(c_{p,f}\ \rho_f\ T)}{\partial t} + (1-\epsilon)\ \frac{\partial(\rho_s\ c_{p,s}\ T)}{\partial t} = \Lambda_{\text{eff}}\ \frac{\partial^2 T}{\partial x_i^2} - u_{f,0,i}\ \frac{\partial(\rho_f\ c_{p,f}\ T)}{\partial x_i} - u_{s,0,i}\ \frac{\partial(\rho_s\ c_{p,s}\ T)}{\partial x_i} + \dot{Q}_R \qquad \text{(eq. 5)}$$

In the equation T is the temperature, Λ_{eff} the effective thermal conductivity and $\dot{Q}_R$ the heat of reaction. The volumetric heat capacity of the solid ($\rho_p\, c_{p,s}$) and of the fluid ($\rho_f\, c_{p,f}$) depend on the water content and are approximated with:

$$\rho_s\, c_{p,s} = \rho_{s,0}\ (c_{p,s,0} + y_s\, c_{p,w}) \quad \Rightarrow \quad \frac{\partial\,(\rho_s\, c_{p,s})}{\partial y_s} = \rho_{s,0}\, c_{p,w} \qquad \text{(eq. 6)}$$

$$\rho_f\, c_{p,f} = \rho_f\ (c_{p,f} + y_f\, c_{p,v}) \quad \Rightarrow \quad \frac{\partial\,(\rho_f\, c_{p,f})}{\partial y_f} = \rho_f\, c_{p,v}$$

with $c_{p,w}$, $c_{p,v}$, $c_{p,s,0}$ and $c_{p,f,0}$ as the specific heat capacity of water, water vapour, of the solid at $y_s = 0$ and of the fluid at $y_f = 0$. The effective mass dispersion coefficient D_{eff} and effective thermal capacity of the fluid Λ_{eff} are calculated according to VDI-Wärmeatlas (Tsotsas, 2002). For the description of the reaction kinetic a linear driving force approach is used:

$$R_s = k_{\text{LDF}}\ (y_s - y_{\text{eq}}) \qquad \text{(eq. 7)}$$

In the equation y_{eq} is the reaction equilibrium and k_{LDF} a linear driving force coefficient which is evaluated according to Gorbach et al. (Gorbach et al., 2004). For the description of the reaction equilibrium y_{eq} in dependency of temperature and water vapour pressure an adsorption model is used. This assumes that these models can also be applied to composites of salt impregnated zeolites. Experimental investigations have shown, that for the material investigated in this study, this assumption is justified. However, with increasing salt concentration on the zeolite particle the adsorption models might lose their validity for the description of the reaction equilibrium and a different approach has to be used.
In this study for the description of the reaction equilibrium the Dubinin-Astakhov equation is applied which is popular for describing micropore filling for many microporous solids (Do, 2008). The heat of reaction $\dot{Q}_R$ in eq. 5 is described by:

$$\dot{Q}_R = \Delta H_R\ R_s\ \rho_{s,0}\ (1-\epsilon) \qquad \text{(eq. 8)}$$

The reaction enthalpy ΔH_R is calculated from the van't Hoff equation.

$$\frac{\Delta H_R}{R_g\, T^2} = -\left(\frac{\partial \ln p_w}{\partial T}\right)_{y_w} \qquad \text{(eq. 9)}$$

For isotherms of the Dubinin-Astakhov type the corresponding equation to express the heat of reaction in terms of conversion can be found in literature (e.g. Do, 2008).

5.2. Results of the numerical investigation

In a first step the general applicability of the simulation model has been validated with measured data of experimental investigations performed in the experimental setup. The adsorption isotherm and the reaction kinetic for a composite, a salt impregnated 4A zeolite (salt concentration of approximately 5 mass percent), have been determined in the fixed bed reactor and implemented in the simulation model. The other parameters such as the effective thermal conductivity or specific heat capacity have been estimated based on data taken from literature. Further experiments have been performed in the experimental setup with varying inflow conditions of the airflow (temperature, water vapour pressure). These experiments have been simulated with the numerical model and the results were compared to the results obtained from the experiments. In figure 6 one of theses experiments as well as the corresponding results of the numerical calculation is shown. Depicted are the measured and calculated water vapour pressure and temperature of the airflow at the reactor inlet and outlet during an exothermic reaction. A very good agreement between measurements and simulation is achieved which verifies the applicability of the model described above.

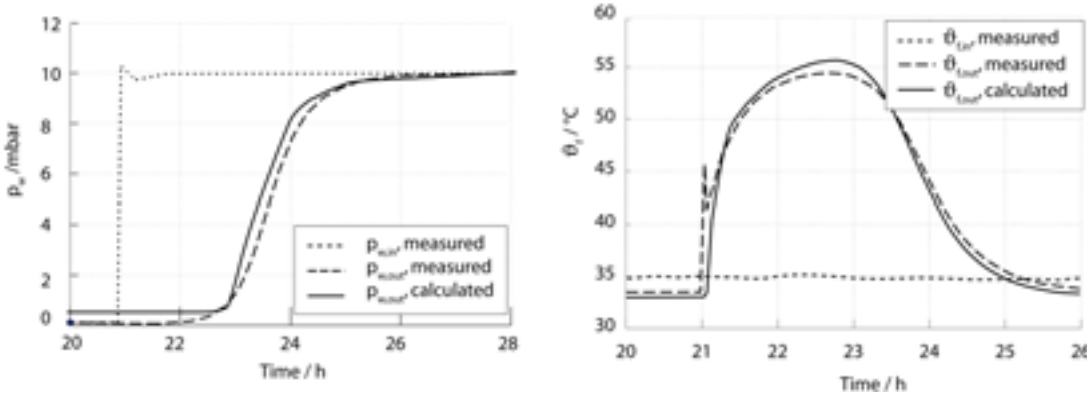

Fig. 6: Exothermic reaction of the composite of 4A zeolite and salt. Left: Water vapour pressure of the airflow at the reactor inlet and outlet (measured and calculated). Right: Airflow temperature at the reactor inlet and outlet (measured and calculated)

Assumptions and boundary conditions for the numerical model

The simulation study aims at deriving a reactor design for a thermo-chemical energy store using a composite of a salt impregnated zeolite as storage material. In a first instance, the main goal is to understand the processes inside the reactor e.g. the reaction behaviour of the material, the temperature distribution inside the reactor and the sensitivity of different reactor designs to a variation in the inflow conditions of the airflow. A precise model of one specific type of a composite, for which detailed information on chemical, physical and thermodynamic properties are required, is not in the primary focus. Hence, several simplifications have been made concerning the material characteristic as well as the flow conditions inside the reactor.

If not otherwise specified the following reactor geometry, boundary and initial conditions have been applied:

- The reactor is rectangular with the following dimensions: height = depth = 0.8 m, width = 0.1 m. The cross-section area for the airflow is $A_f = 0.64\,m^2$ (depth x height).
- A two-dimensional model is applied, hence variation along the reactor depth are neglected.
- The fluid is entering the reactor from lateral at an inlet temperature of $\vartheta_{f,in} = 35\,^\circ$ C and an absolute humidity of $x_{f,in} = 6\,g\,kg^{-1}$. The volume flow is constant with $\dot{V}_f = 180\,m^3\,h^{-1}$.
- The material is entering the reactor from vertical (cross flow reactor) or is stationary inside the reactor (fixed bed reactor). The inlet or initial temperature of the material is ϑ= 35 ° C. The material is entering the reactor (cross-flow) or has an initial conversion (fixed bed reactor) of $y_s = 0.02$.
- The material has a uniform particle size of 2 mm.

- The coefficients of the Dubinin-Astakhov equation have been adapted to the adsorption isotherms of the composite described in section 4. The reaction kinetic coefficient k_{LDF}, effective mass dispersion coefficient D_{eff} and thermal conductivity coefficient Λ_{eff} have been adopted from the numerical model of the salt impregnated 4A zeolite.
- The temperature dependency of the thermal conductivity and of the specific heat capacity is neglected.

5.2.1. Cross flow reactor

The reaction in the cross flow reactor is a stationary process. Hence, in the mass and energy balance (eq. 2, eq. 3, eq. 5) the derivative with respect to time is zero. In figure 7 results obtained from the numerical simulation are depicted.

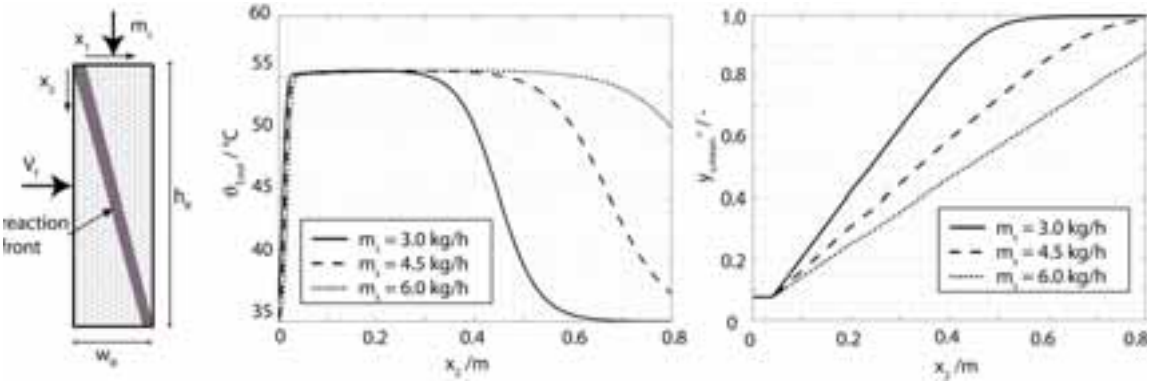

Fig. 7: Results of the numerical simulation of the cross flow reactor design. Left: Outlet temperature of the airflow in dependency of the reactor height. Right: Fractional conversion of the material averaged over the reactor width in dependency of the reactor height

The left diagram depicts the outlet temperature of the airflow over the reactor height, the right diagram the fractional conversion of the material averaged over the reactor width. In the cross-flow reactor the reaction front is stationary, going diagonally from the material / air inlet (upper left corner in figure 7) to the material / air outlet (lower right corner in figure 7). The conversion front has the same shape with unreacted material in the upper right region and reacted material in the lower left region. For the presentation of the material conversion over the reactor height, a mean conversion $y^+_{s,mean}$ over the reactor width w_R has been calculated:

$$y^+_{s,mean} = \frac{1}{w_R} \int_{x_1=0}^{x_1=w_R} y^+_s \, d\, x_1 \qquad\qquad y^+_s = \frac{y_s}{y_{s,ref}} \qquad \text{(eq. 10)}$$

with the fractional conversion y^+_s defined as the conversion of the material y_s related to the maximum possible conversion at reference conditions $y_{s,ref}$. Similar, the mean outlet temperatur of the airflow is determined by averaging the temperature over the reactor height h_R:

$$\vartheta_{f,mean} = \frac{1}{h_R} \int_{x_2=0}^{x_2=h_R} \vartheta_f d\, x_2 \qquad \text{(eq. 11)}$$

At the material inlet ($x_2 = 0$) the material is entering the reactor at an initial conversion of $y_s = 0.02$. Along the reactor height the material is reacting with the water vapour from the airflow until complete conversion is achieved, or, if not enough water vapour is available, until the material is leaving the reactor at the material outlet. The heat energy released during the exothermic reaction is transported out of the reactor by the airflow. With increasing conversion of the material the reaction rate decreases and less heat of reaction is released. This results in a decreasing temperature of the airflow along the reactor height.

At a comparatively high mass flow of the material ($\dot{m}_s = 6.0\,\mathrm{kg\,h^{-1}}$) complete conversion of the material is not achieved at the material outlet. The material is leaving the reactor with a fractional conversion of

$y^+_{s,mean} < 1$. As there is still reaction in regions near the material outlet the reactor temperature maintains high and the air is leaving the reactor with a relatively high temperature (mean outlet temperature of $\vartheta_{mean,out} = 54.4\,°C$). If the mass flow of the material is too low ($\dot{m}_s = 3.0\,kg\,h^{-1}$) full conversion is already achieved at a reactor height of $x_2 = 0.5\,m$. As there is no reaction of the material further downstream the outlet temperature of the airflow decreases with increasing reactor height. The airflow is leaving the reactor with a mean outlet temperature of $\vartheta_{mean,out} = 46.3\,°C$. The optimal mass flow of the material under the inflow conditions of the air is $\dot{m}_s = 4.5\,kg\,h^{-1}$. Almost full conversion of the material is achieved at the material outlet ($y^+_{s,mean} = 0.99$) and at the same time the air is leaving the reactor at a comparatively high outlet temperature of $\vartheta_{\mathrm{mean,out}} = 51.7\,°$ C. In table 1 the main results of the cross flow reactor design are summarized. The thermal power output $\dot{Q}_{th}$ provided by the airflow is calculated according to eq. 12:

$$\dot{Q}_{th} = \dot{m}_f\, c_{p,f}\, (\vartheta_{f,mean,out} - \vartheta_{f,in}) \qquad \text{(eq. 12)}$$

In the equation $\dot{m}_f$ is the mass flow of the air, $\vartheta_{f,mean,out}$ the mean outlet temperature of the airflow and $\vartheta_{f,in}$ the inlet temperature of the airflow. The specific thermal energy density provided by the airflow is defined with:

$$q_{th} = \frac{\dot{Q}_{th}}{\dot{m}_s} \qquad \text{(eq. 13)}$$

The quantity q_{th} is a measure for the usable energy storage density of the material.

Tab. 1: Main results of the numerical investigation of the cross flow reactor

$\dot{m}_s$ kg h^{-1}	y^+ %	$\vartheta_{\mathrm{f,mean,out}}$ ° C	$\dot{Q}_{th}$ kW	q_{th} kWh kg^{-1}
3.0	100.0	46.3	0.77	0.220
4.5	98.9	51.7	0.99	0.220
6.0	87.4	54.5	1.16	0.193

The simulation study shows that full conversion of the material has to be achieved at the material outlet in order to make use of the complete specific energy density of the material. This implies that the material mass flow has to be adapted to the inflow conditions of the airflow, mainly to the water vapour supply into the reactor.

5.2.2. Fixed bed reactor

In the fixed bed reactor the material is stationary inside the reactor and the convective term for the bulk velocity $u_{s,0}$ in eq. 3 and eq. 5 are set to zero. Figure 8 shows the fractional conversion y^+_s of the material (left) and the temperature of the airflow ϑ_f (right) over the reaction time for different positions along the reactor width. With increasing reaction time the reaction front is moving through the reactor from the airflow inlet to the airflow outlet. The breakthrough curve of the temperature and of the material conversion follow the reaction front. During the reaction an overall heat of $Q_{th} = 10.6\,kWh$ is released. This corresponds to a specific energy density of $q_{th} = 0.23\,kWh\,kg^{-1}$.

However, not the complete heat provided by the reaction can be used for further processes e.g. for transferring the heat to the water circuit via the air to water heat exchanger. When the reaction front is approaching the airflow outlet, most of the material is already reacted and the reaction rate decreases. This results in less heat released during the reaction and the airflow outlet temperature decreases. Assuming that a minimum temperature lift of the airflow of $\Delta T = 10\,K$ is required in the air to water heat exchanger, a useful heat of reaction of $Q_{th} = 9.8\,kWh$ or specific energy of $q_{th} = 0.21\,kWh\,kg^{-1}$ is released. The material has to be replaced after a reaction time of 9 hours and a fractional conversion of the material averaged over the complete reactor of $y^+_{mean} = 0.94$ is achieved.

5.2.3. Quasi-continuous cross flow reactor

Both concepts, the cross flow reactor and the fixed bed reactor, show a very good performance in terms of thermal power output and conversion of the material. A drawback of the fixed bed reactor is the

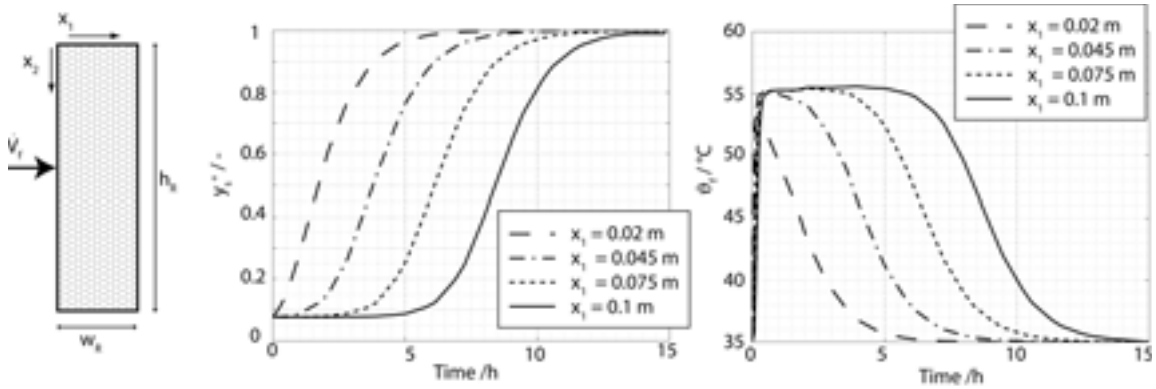

Fig. 8: Simulation results of the fixed bed reactor. Left: Conversion of the material at different positions along the reactor width in dependency of the reaction time. Right: Airflow temperature at different positions along the reactor width in dependency of the reaction time.

instationary thermal power output of the reactor resulting from a decreasing temperature of the airflow with increasing conversion of the material. As a minimum temperature lift is required in the air to water heat exchanger, the material inside the reactor has to be replaced before full conversion is achieved. In this study, in the fixed bed reactor an average fractional conversion of $y^+ = 0.94$ is achieved when a minimum temperature lift of the airflow of $\Delta T = 10\,\mathrm{K}$ is required. In the cross flow reactor, a fractional conversion of $y^+ = 0.99$ is obtained at a constant outlet temperature of the airflow with a temperature lift of $\Delta T = 17\,\mathrm{K}$. However, the cross-flow reactor design has high demands on the reaction control. A uniform material flow at very low bulk velocities has to be guaranteed. Furthermore the mass flows of the material flow and airflow (or rather water vapour flow) have to be optimally adjusted with one another. A too high mass flow ratio of the material flow to the air flow results in an uncompleted conversion at the material outlet; a too low mass flow ratio results in a comparatively low temperature lift of the airflow. Here, the fixed bed reactor design has advantages as the material is stationary inside the reactor. This simplifies the reaction control and in addition no technical measures have to be taken for a unifom mass flow.

To make use of the strengths of both reactor concepts, a quasi-continuous cross flow reactor was developed. A sketch of this reactor design is depicted in figure 9. At the material outlet the reactor width is reduced which results in a higher airflow in this region as the flow resistance is reduced. The reaction is performed in a fixed bed, meaning no movement of the material. With increasing reaction time the material in the lower part of the reactor is already reacted whereas in the upper part of the reactor most of the material is still unreacted. After a certain reaction time (e.g. when the temperature T_1 is dropping below a limit value) the material in the lower part of the reactor is removed and new material is entering the reactor from top. The reaction is continued in a fixed bed until the temperature T_1 is below the limit value.

Figure 9 shows first results of numerical investigations. In this study a fixed bed operation of the reactor has been analysed without any discharging of the material. The simulation was performed for a reactor of the following dimensions: height = depth = 0.8 m, width (material inlet) = 0.1 m, width (material outlet) 0.06 m. The same initial and inlet condition for the material and airflow as for the fixed bed reactor apply.

The figure shows the temperature T_1 at $x_2 = 0.75\,\mathrm{m}$, T_2 at $x_2 = 0.3\,\mathrm{m}$ of the airflow and the thermal power output $\dot{Q}_{th}$ provided by the airflow. With increasing reaction time, the temperature T_1 decreases whereas the temperature T_2 remains on a high level for a comparatively long time. This results in only a slight decrease of the thermal power output from approximately $\dot{Q}_{th} = 1200\,\mathrm{W}$ to $\dot{Q}_{th} = 950\,\mathrm{W}$. When the temperature at T_1 is dropping below a limit value, the material in the lower part of the reactor has to be replaced. In this example, if the material in the lower part of the reactor was replaced after 5.5 hours, the replaced material would have a fractional conversion of $y_s^+ = 0.99$. At this time the mean outlet temperature of the airflow is $\vartheta_{mean,out} = 50.9\,^\circ\mathrm{C}$, equivalent to a temperature lift of the airflow over the reactor of $\Delta T = 15.9\,\mathrm{K}$. This shows that similar to the cross-flow reactor design a very high fraction of the energy storage density of the material can be utilized.

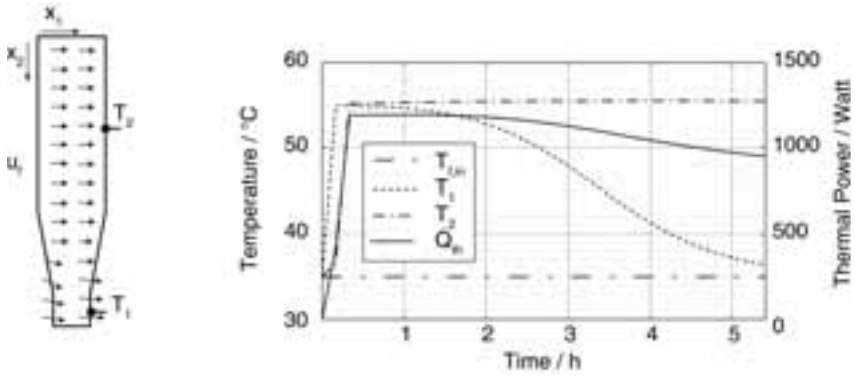

Fig. 9: Sketch of the reactor design of the quasi-continuous cross flow reactor (left). Results of the numerical simulation of the quasi-continuous cross flow reactor during fixed bed operation (no replacement of the material) (right).

Since the results determined for the newly developed quasi-continous cross flow reactor are quite promising this concept will be further investigated. As next steps further numerical and experimental investigations will be performed to analyse the reactor design under instationary operation conditions.

6. Summary

A process design, the CWS-NT-concept for a thermo-chemical energy store integrated in a solar thermal system has been presented in this paper. An essential part of the thermo-chemical energy store is the reactor where the heat and mass transfer take place. In this paper several external reactor designs for a thermo-chemical energy store are presented. A characteristic feature of external reactor designs is the transport of the material from and to the reactor as the external reactor is seperated from the material reservoir. To analzye the processes inside the reactor, detailed numerical investigations with the finite element simulation software "COMSOL Multiphysics" have been performed for a fixed bed reactor and a cross flow reactor. Focus of the simulation study is to understand the processes in the reactor during the exothermic reaction of a composite (salt impregnated zeolite) with humid air. An important criterium, which has to be fulfilled by the reactor, is that a high fraction of the energy density of the material can be used for further processes. This implies a minimum temperature lift of the airflow to be ensured during reaction.

Strenghts and weaknesses of the different reactor concepts have been demonstrated through results from numerical simulation studies. At optimal operation conditions of the reactor - meaning an optimal mass flow ratio of the water vapor transported into the reactor via the air to the material massflow - the cross flow reactor design is superior to the fixed bed reactor design in terms of the specific thermal energy density released during the reaction. However, the cross flow reactor design has high demands on the reaction control due to the sensitivity of the reaction to a variation in the air inflow conditions. In addition, a uniform mass flow inside the reactor at very low bulk velocities has to be guaranteed but is technically difficult to realize. Based on these considerations a quasi-continuous cross-flow reactor design has been developed. Instead of a continuous material mass flow through the reactor, as in the cross flow reactor design, the material is removed discontinously from the reactor. In the lower part of the reactor, near the material outlet, a faster conversion of the material is achieved compared to the materials in the upper part, by reducing the width of the reactor and hence increasing the amount of air passing this part of the reactor. When full conversion is achieved in the area near the material outlet, the material outlet opens and part of the material is removed. At the same time the reactor is refilled with unreacted material from the top. First simulation studies show that a high fractional conversion of the material can be achieved and, at the same time, the temperature lift of the airflow leaving the reactor is only slightly decreasing with increasing reaction time. This indicates a very efficient process design where a high fraction of the specific energy density of the material can be utilized. Further experimental and numerical investigations are in progress to analyze the reactor design under varying operating conditions in more detail.

Experimentel investigation on materials for thermo-chemical energy storages have been conducted. Com-

posite materials of salt impregnated zeolites exhibit very good properties in terms of thermal performance (reaction kinetic, specific thermal energy storage density) and mechanical and thermal stability (transportable, low thermal degradation). Both criteria are crucial for the use in a thermo-chemical energy store. Further investigation are on-going and it is expected that a huge increase in the specific thermal energy density can be achieved by improving the material structure and the material production process.

Nomenclature and Symbols

Symbol	Unit	Quantity
A	m^2	cross-section area
$A_{(s)}$		solid reactant
$B_{(s)}$		solid reaction product
c_p	$J\,kg^{-1}\,K^{-1}$	specific heat capacity
D_{eff}	$m^2\,s^{-1}$	effective mass dispersion coefficient
ΔH_R	$J\,kg^{-1}$	reaction enthalpy
h_R	m	reactor heigth
k_{LDF}	s^{-1}	linear driving force coefficient
m_s	kg	solid mass
p_0	mbar	system pressure
p_w	mbar	water vapor pressure
Q_{th}	J	thermal energy
$\dot{Q}_{th}$	W	thermal power output
$\dot{Q}_R$	$W\,m^{-3}$	heat of reaction
q_{th}	$J\,kg^{-1}$	specific thermal energy
R	s^{-1}	reaction rate
R_g	$J\,mole^{-1}\,K^{-1}$	gas constant
T	K	temperature
t	s	time
u_0	$m\,s^{-1}$	superficial velocity
w_R	m	reactor width
x_i	m	coordinate in direction i, $i = 1, 2$

Symbol	Unit	Quantity
y_s	-	conversion of the material
y_w	-	absolute humidity of the airflow
y_s^+	-	fractional conversion of the material
Greek letters		
ϵ	-	bed porosity
ϑ	°C	temperature
Λ_{eff}	$W\,m^{-1}K^{-1}$	effective thermal conductivity
ρ	$kg\,m^{-3}$	density
Indices		
0		initial, unreacted
f		fluid
g		gas
in		inflow
eq		equilibrium
mean		mean
out		outflow
ref		reference
s		solid
w		water
v		vapour

References

Bertsch, F., Kerskes, H., Drück, H., and Müller-Steinhagen, H. (2010). Materialuntersuchung für chemische Langzeitwärmespeicher. In *Tagungsband. OTTI. 20. Symposium Thermische Solarenergie*, pages 258 – 663. ISBN: 978-3-941785-29-8.

Brunauer, S., Emmett, P. H., and Teller, E. (1938). Adsorption of gases in multimolecular layers. *Journal of the American Chemical Society*, 60(2):309–319.

Comsol (2010). *COMSOL Multiphysics 4.1 Installation and Operation guide.* Comsol Multiphysics GmbH, Stockholm, Sweden.

Do, D. D. (2008). *Adsorption Analysis: Equilibria and Kinetics (V2)*, volume 2 of *Series on Chemical Engineering*. Imperial College Press.

Gorbach, A., Stegmaier, M., and Eigenberger, G. (2004). Measurement and modeling of water vapor adsorption on zeolite 4a - equilibria and kinetics. *Adsorption*, 10:29–46.

Kerskes, H., Bertsch, F., Mette, B., Wörner, A., and Schaube, F. (2011a). Thermochemische Energiespeicher. *Chemie Ingenieur Technik*, 83, to be published.

Kerskes, H., Mette, B., Bertsch, F., Asenbeck, S., and Drück, H. (2011b). Development of a thermo-chemical energy storage for solar thermal applications. In *Proceedings. ISES, Solar World Congress Proceedings, 2011, Kassel.*

Tsotsas, E. (2002). Wärmeleitung und Disperion in durchströmten Schüttungen. In *VDI Wärmeatlas (2010)*. Verein Deutscher Ingenieure.

The work described in this paper is part of the project "Chemische Wärmespeicherung mittels reversibler Feststoff-Gasreaktionen (CWS)" funded by the BMWi (Bundesministerium für Wirtschaft und Technologie, German Federal Ministry of Economics and Technology) under the grant number 0327468B and managed by PtJ (Projektträger Jülich, Project Management Jülich). The authors gratefully acknowledge this support. The sole responsibility for the content of this document lies with the authors.